B-SPLINES COLLOCATION FOR PLATE BENDING EIGENANALYSIS

Christopher G. Provatidis

msp

B-SPLINES COLLOCATION FOR PLATE BENDING EIGENANALYSIS

CHRISTOPHER G. PROVATIDIS

Following the recent encouraging findings in the area of 2-D acoustics, this paper investigates the performance of a B-spline collocation method in the extraction of natural frequencies (eigenvalue analysis) of thin plates in bending. Numerical formulation and associated results refer to uniformly discretized rectangular and circular plates, for which closed-form analytical or approximate solutions are available in the literature. The computational results show that the proposed B-spline collocation method is of higher quality than the previously known cubic B-splines Galerkin–Ritz formulation; both of them converge more rapidly to the accurate solution than what the conventional finite element method does for the same mesh density.

1. Introduction

Engineering analysis of arbitrarily shaped or arbitrarily loaded structures is usually performed using the well-known finite element method (FEM) [Bathe 1996]. Particularly in mechanical engineering, where the structural components generally consist of free shaped boundaries produced by a CAD system, it is more convenient to deal with their B-splines representation [de Boor 1972; Farin et al. 2002; Piegl and Tiller 1995]. In addition to a CAD model, computational engineering analysis (CAE) can be performed on the basis of either B-splines [Höllig 2003] or NURBS [Cottrell et al. 2009]. For a detailed review on the CAD/CAE integration, the interested reader may consult [Provatidis 2013].

B-splines based finite elements have been extensively used in the finite element praxis. In more detail, structural engineering applications cover static, dynamic and stability analyses [Peng-Cheng et al. 1987; Akhras and Li 2011]; an older survey is [Grigorenko and Kryukov 1995]. A great number of papers on B-splines finite element models applied to plates and shells have been published in the last twenty years. These include isotropic [Antes 1974; Gupta et al. 1991; Fan and Luah 1995], orthotropic [Cheng and Dade 1990], cross- and angle-ply multilayered laminated [Patlashenko and Weller 1995; Dawe and Wang 1995; Kolli and Chandrashekhara 1997; Reddy and Palaninathan 1999; Park et al. 2008; Kapoor and Kapania 2012; Golmakani and Mehrabian 2014], functional graded materials (FGM) [Valizadeh et al. 2013; Tran et al. 2013] and shell [Echter et al. 2013] structures, among others. A tendency of the last few years is to combine B-splines with wavelet ideas [Han et al. 2007; Zhang et al. 2010; Li and Chen 2014].

Despite the aforementioned progress, it has been reported that the computer effort required to estimate the matrices of these CAD-based macroelements (in potential and structural problems) is relatively high [Provatidis 2004; 2012]. As a remedy to this shortcoming, in 2005 the author proposed preserving the global CAD-based interpolation but substituting the Galerkin–Ritz formulation (which needs domain integration to estimate the mass and stiffness matrices) by a global collocation scheme [Provatidis 2006,

p. 6704]. Similar numerical results were later reported for the particular case of a (NURBS-based) isogeometric analysis [Hughes et al. 2010].

So far, the above idea of global collocation has been successfully applied to the static analysis of 2-D structures [Provatidis 2008b; 2009; Provatidis and Ioannou 2010], eigenvalue analysis of 1-D elastic rods [Provatidis 2008a], as well as the eigenanalysis of 2-D acoustic cavities [Provatidis 2014] and 2-D elastic structures [Filippatos 2010]. Later, isogeometric collocation methods were proposed [Auricchio et al. 2010]. Nevertheless, an application of this idea to thin plate bending is still missing.

Within this context, this paper preserves the aforementioned idea of approximating the deflection $w(x, y)$ within the plate through a B-splines tensor product but replaces the Galerkin–Ritz computational procedure with a global collocation method (GCM), thus avoiding domain integration. The cost of this facility is the increase of the polynomial degree from $p = 3$ to higher values ($p \geq 5$). The proposed methodology is successfully tested in a square plate (simply supported, clamped), as well as in a clamped circular plate.

2. Governing equations and numerical solution

The partial differential equation of motion for a plate in bending is given by

$$D\nabla^4 w(x, y, t) + \rho h \frac{\partial^2 w(x, y, t)}{\partial t^2} = f(x, y, t), \tag{1}$$

where D is the flexural rigidity, ρ is the mass density, h is the plate thickness, and f is the loading towards the z-direction.

Following [Antes 1974; Höllig 2003], the deflection is expanded into a B-splines tensor product of the form

$$w(x, y; t) = \sum_{i=1}^{n} \sum_{j=1}^{m} N_{i,p_n}(x) \cdot N_{j,p_m}(y) \cdot a_{ij}(t), \quad i = 1, \ldots, n; \ j = 1, \ldots, m, \tag{2}$$

where $N_{i,p_n}(x)$ and $N_{j,p_m}(y)$ are the basis functions in the x- and y-direction, respectively. The aforementioned basis functions (B-splines) are *piecewise* polynomials of p_n-th and p_m-th degree, respectively, and are characterized by compact support [Piegl and Tiller 1995]. Further details are given in Section 3.1.

It is noted that the integers n and m in (2) represent the number of *control* points in the x- and y-direction, respectively, whereas for the degrees of the corresponding polynomials, $p_n < n$ and $p_m < m$ (see (8) below).

According to the *global collocation method* [Provatidis 2008a; 2008b; 2009; Provatidis and Ioannou 2010; Filippatos 2010], a certain number of n_c collocation points (x_c, y_c) are chosen, at which the governing equation is satisfied as follows:

$$D \cdot \nabla^4 \left[\sum_{i=1}^{n} \sum_{j=1}^{m} N_{i,p_n}(x_c) \cdot N_{j,p_m}(y_c) \right] \cdot a_{ij}(t) + \rho h \cdot \sum_{i=1}^{n} \sum_{j=1}^{m} N_{i,p_n}(x_c) \cdot N_{j,p_m}(y_c) \cdot \ddot{a}_{ij}(t) = f(t). \tag{3}$$

Setting

$$k_{c,ij} = D \cdot \nabla^4 [N_{i,p_n}(x_c) \cdot N_{j,p_m}(y_c)] \tag{4}$$

and

$$m_{c,ij} = \rho h \cdot [N_{i,p_n}(x_c) \cdot N_{j,p_m}(y_c)], \tag{5}$$

(3) obtains the matrix form

$$[M] \cdot \{\ddot{a}(t)\} + [K] \cdot \{a(t)\} = \{f(t)\}. \tag{6}$$

In this way, mass and stiffness matrices of dimensions $n_c \times (nm)$ are produced.

In the general case, unlike the finite element method, the aforementioned matrices are not square before the boundary conditions are imposed. Imposing the prescribed values (flexural displacements or slopes) along the contour of the plate, we have to proceed so as to derive square matrices at the end. To this purpose, the proper choice of collocation points is demanded.

3. Global approximation

3.1. *One-dimensional B-spline approximation.* For the sake of completeness, in the following text, de Boor's procedure is briefly exposed.

For a given polynomial degree p, the construction of a B-spline along a straight line segment is based on a nondecreasing sequence of $q + 1$ *breakpoints* $(x_0, x_1, \ldots, x_{q-1}, x_q)$, i.e., the two ends (x_0, x_q) as well as $(q - 1)$ internal breakpoints $(x_1, \ldots, x_{q-1})$. Assuming a certain multiplicity for the inner knots, say μ, they compose the so-called *knot vector*,

$$V = \left\{ \underbrace{x_0, \ldots, x_0}_{p+1}, \underbrace{x_1, \cdots, x_1}_{\mu}, \ldots, \underbrace{x_{q-1}, \cdots, x_{q-1}}_{\mu}, \underbrace{x_q, \ldots, x_q}_{p+1} \right\} \tag{7}$$
$$= \{v_0, v_1, \ldots, v_{\mu(q-1)+2p+1}\}.$$

The following facts are well known:

(1) The above $\mu(q - 1) + 2(p + 1)$ elements in the vector V are associated to

$$n_{\text{CTRL}} = \mu(q - 1) + (p + 1) \tag{8}$$

control points [de Boor 1972; Farin et al. 2002; Piegl and Tiller 1995].

(2) The basis functions, $N_{i,p}(x)$, have the partition of unity property,

$$\sum_{j=0}^{q} N_{j,p}(x) = 1. \tag{9}$$

For a straight side (e.g., AB in the real domain Ω), the control points belong to the side while for a curved side they do not, except for the first (P_0) and last (P_n). In other words, the end segments of the polygon $P_0 P_1 \ldots P_{n-1} P_n$ (called the *generator*) are tangent to the curved side AB at end nodes P_0 and P_n. Details can be found elsewhere, for example, in [Farin et al. 2002].

The i-th B-spline function of p-degree, denoted by $N_{i,p}(x)$, is defined as follows (see for example

[Piegl and Tiller 1995, p. 50]):

$$N_{i,0}(x) = \begin{cases} 1, & \text{if } v_i \leq x < v_{i+1}, \\ 0, & \text{otherwise,} \end{cases} \tag{10}$$

$$N_{i,p}(x) = \frac{x - v_i}{v_{i+p} - v_i} N_{i,p-1}(x) + \frac{v_{i+p+1} - x}{v_{i+p+1} - v_{i+1}} N_{i+1,p-1}(x). \tag{11}$$

Similarly, the first derivative of $N_{i,p}(x)$ can be effectively calculated by the recursion [Piegl and Tiller 1995, p. 59]

$$N'_{i,p}(x) = \frac{p}{v_{i+p} - v_i} N_{i,p-1}(x) - \frac{p}{v_{i+p+1} - v_{i+1}} N_{i+1,p-1}(x), \tag{12}$$

whereas similar recursive expressions can be obtained for higher derivatives.

3.2. *Two-dimensional B-spline approximation: tensor product.* Let us consider a mapping from the real xy-domain (ABCD) to the reference $\xi\eta$-square (A′B′C′D′) in which $0 \leq \xi$, $\eta \leq 1$. The axis origin is chosen at the corner A (resp. A′), whereas the normalized axes ξ and η lie on the sides A′B′ and A′D′, respectively. Without loss of generality, the sides (AB, CD) and (A′B′, C′D′) as well as (B′C′, D′A′) and (BC, DA) are uniformly divided into n_ξ and n_η segments, respectively, thus introducing a mesh of $(n_\xi + 1) \times (n_\eta + 1)$ *breakpoints* (Figure 1).

Although the below illustrated B-spline macroelement reminds us of the classical Lagrangian type element [Bathe 1996, pp. 344, 456], it highly differs from it for the following reasons. Based on the aforementioned uniformly distributed breakpoints ($\xi = 0, \xi_1, \ldots, 1$; $\eta = 0, \eta_1, \ldots, 1$), each of the first two opposite sides AB and CD (parallel to x-axis) are described through n control points fulfilling the formula

$$n = \mu(n_\xi - 1) + (p_n + 1), \tag{13}$$
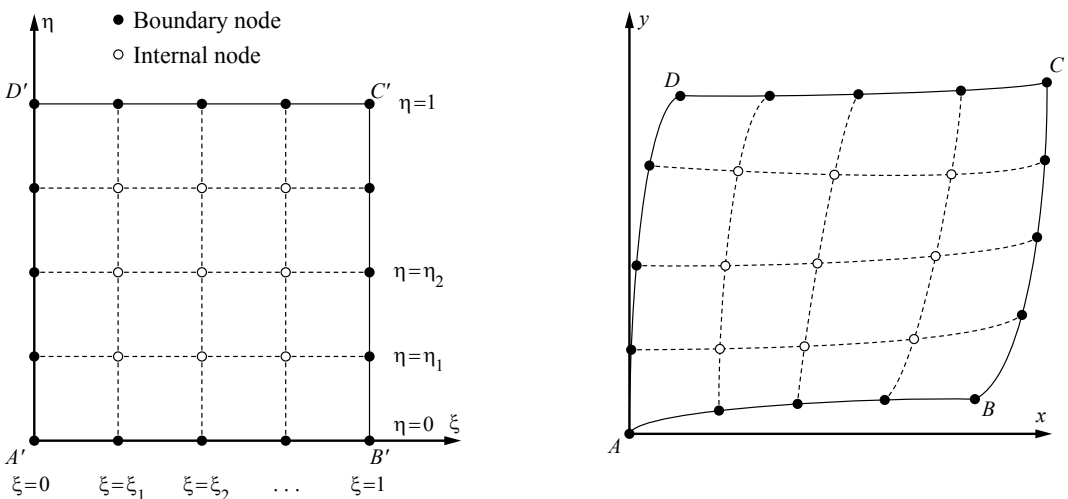
Figure 1. Uniformly arranged breakpoints of a B-splines plate-bending macroelement in the normalized, left, and the real domain, right (only the breakpoints are shown).
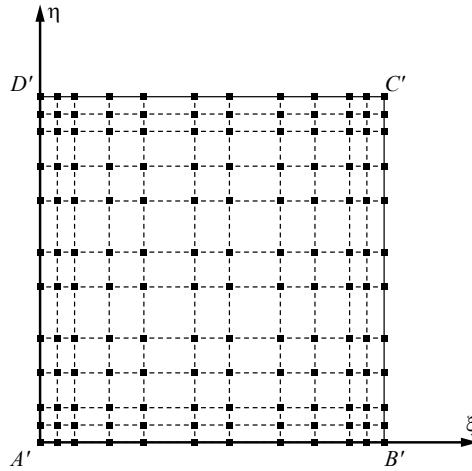
Figure 2. True position of the $\bar{q} = n \times m = 12 \times 12$ control points that correspond to the uniformly distributed breakpoints shown in Figure 1, left (number of segments $n_\xi = n_\eta = 4$; polynomial degree: $p = 5$).

while the other two opposite sides BC and DA (parallel to y-axis) are described through m control points

$$m = \mu(n_\eta - 1) + (p_m + 1). \tag{14}$$

Concerning the normalized (reference) element shown in Figure 1, left, the n control points belong to the straight line A′B′ and another set of n control points belong to the straight line D′C′. Similarly, the m control points belong to the straight line B′C′ and another set of m control points belong to the straight line A′D′. In contrast, in the real domain (let us consider, for example, the side AB: Figure 1, right) the *first* and *last* control points *coincide* with the *corner* points A and B respectively (ends of curve AB); however, the other control points may or may not belong to the curve AB (they may be found inside or outside the domain ABCD).

Returning to the normalized reference element (Figure 2), the mesh required for the B-spline representation of the patch geometry consists of $\bar{q} = nm$ control points, produced as the tensor product of n by m ones.

Each of the aforementioned control points, say the I-th, is associated with one global shape function given by

$$\phi_{I,\text{B-splines}}(\xi, \eta) = N_{i,p_n}(\xi) \cdot N_{j,p_m}(\eta), \quad \begin{cases} I = 1, \ldots, \bar{q} \equiv n \times m, \\ i = 1, \ldots, n; \ j = 1, \ldots, m. \end{cases} \tag{15}$$

Although the values of p_n and p_m may be different from one another, henceforth we take the same polynomial degree, that is $p_n = p_m = p$.

3.3. *Collocation points*. In order to determine the proper number of collocation points in each direction, it is necessary to assign values first to the polynomial degree p and then to the multiplicity of inner knots μ. It is well known that for every value of μ, the solution $w(x, y)$ is characterized by $C^{p-\mu}$-continuity.

According to (13), the number of control points towards a certain direction, say the ξ-direction, in which n_ξ subdivisions exist is $n = \mu(n_\xi - 1) + (p + 1)$. The four boundary conditions (for example, two fixed ends) reduce the number of total degrees of freedom by four, and therefore the remaining unknown coefficients will be $(n - 4)$. If within each of the n_ξ segments (defined between any two successive breakpoints) a number of c collocation points are considered, one should obtain so many equations at the c corresponding collocation points as the number of the unknowns, that is: $cn_\xi = n - 4$, whence

$$c = (n - 4)/n_\xi. \tag{16}$$

Substituting (13) into (16), one finally obtains

$$c = \mu + (p - \mu - 3)/n_\xi. \tag{17}$$

Since c must be an integer, we select the nominator in the second adding term of (17) to vanish, whence the multiplicity is given by

$$\mu = p - 3, \tag{18}$$

whence the number of collocation points in ξ-direction will be

$$c = p - 3. \tag{19}$$

Since the partial differential equation (1) is of fourth order, the minimum acceptable polynomial degree is $p = 5$, for which *double* knots ($\mu = 2$) and also $c = 2$ collocation points per direction are needed. Following previous studies in 1-D elliptic problems [de Boor and Swartz 1973], in the case of $p = 5$ the position of the collocation points within any cell of neighboring breakpoints was taken to be identical with those integration points used in a usual 2×2 Gaussian quadrature scheme.

In general, for every $p > 5$, the knot vector is built using $\mu = p - 3$ multiple inner knots, see (7), whereas a Gaussian quadrature scheme of $c \times c = (p - 3) \times (p - 3)$ collocation points per cell is adopted.

Remark. Due to (18), the above choice ($p - \mu = 3$) ensures a numerical solution characterized by C^3-continuity. This means that the deflection w, slope w', bending moment EIw'', and shear force EIw''' are continuous at all inner breakpoints.

Except for the above-mentioned Gaussian points, as also reported in 2-D acoustics (see [Provatidis 2014]), other sets of collocation points such as Demko and Greville ones can be used as well. Nevertheless, despite the global character of these abscissae, no significant influence on the numerical solution has been noticed so far (see Figure 5).

3.4. *Isoparametric approximations.* Tensor products of B-splines are based on the following series expansion ($\phi_j = \phi_{I,\text{B-splines}}$):

$$x(\xi, \eta) = \sum_{j=1}^{\bar{q}} \phi_j(\xi, \eta) \cdot x_j, \quad y(\xi, \eta) = \sum_{j=1}^{\bar{q}} \phi_j(\xi, \eta) \cdot y_j, \quad w(\xi, \eta) = \sum_{j=1}^{\bar{q}} \phi_j(\xi, \eta) \cdot a_j, \tag{20}$$

where a_j are generalized coefficients and *not* the nodal values of deflection w at the $\bar{q}$ control points. Only at the very ends of the boundary the extreme control points (P_0 and P_n) coincide with the corresponding ends of polygon curves (generator).

4. Imposition of Neumann boundary conditions

In contrast to the Dirichlet boundary conditions (b.c.), i.e., $w = 0$, which are imposed merely by deleting the columns that correspond to the restricted degree of freedom (DOF), the Neumann b.c. require a special treatment. In order to demonstrate the procedure, it is more instructive to deal with a clamped beam, and then extend the methodology to a real 2-D plate.

Within this context, let us assume a beam AB of length L, which is clamped at its left end (namely A) whereas the other end (namely B) is free to vibrate. The beam is discretized by B-splines using a number of breakpoints (like those arranged along the edge A′B′ of the square of Figure 2), which correspond to n control points. These control points are associated to the following generalized coefficients: $a_0 = w_0 = w(0)$, $a_1, \ldots, a_{n-1}$, $a_n = w_n = w(L)$. It is efficient to apply the local support property, according to which the basis function $N_{i,p}(x) = 0$ if x is outside the knot interval $[x_i, x_{i+p+1})$. After having constructed the matrices (K, M), which initially are of size $n_c \times n$, the following boundary conditions have to be considered.

Fixed point A:

$$w(0) = N_0(0)a_0 = 0 \tag{21a}$$

and

$$w'(0) = N_0'(0)a_0 + N_1'(0)a_1 = 0. \tag{21b}$$

Since $N_0(0) = 1 \neq 0$, (21a) implies

$$a_0 = 0. \tag{21c}$$

Substituting (21c) into (21b) by virtue of $N_1' \neq (0)$ gives

$$a_1 = 0. \tag{21d}$$

Therefore, the first and second columns of the matrices (K, M) should be deleted, because their elements are multiplied by the null values of the two restrained DOF at the end A (i.e., $a_0 = a_1 = 0$). Therefore, the number of the so far remaining columns (and the associated coefficients a_i) becomes $n - 2$.

Furthermore, concerning the load-free end B, the zero values of the bending moment $w''(L) = 0$ and the shear force $w'''(L) = 0$ have to be imposed. This is easily accomplished by taking into consideration the local support property for the control point B at $x = L$:

$$w''(L) = N_{n-2}''(L)a_{n-2} + N_{n-1}''(L)a_{n-1} + N_n''(L)a_n, \tag{21e}$$

$$w'''(L) = N_{n-3}'''(L)a_{n-3} + N_{n-2}'''(L)a_{n-2} + N_{n-1}'''(L)a_{n-1} + N_n'''(L)a_n. \tag{21f}$$

Equations (21e) and (21f) induce two linear dependencies between the remaining $(n - 2)$ generalized coefficients of the vector a. As a result, the final size of the matrices will be $n_c \times (n - 4)$, and (16)–(19) ensure that $(K_{\text{final}}, M_{\text{final}})$ will be square.

For a uniform arrangement of the breakpoints, and for any polynomial degree p, after some symbolic manipulation it is found that $N_{n-2}''(L) = N_n''(L) = -2N_{n-1}''(L)$; therefore (21e) implies

$$a_{n-1} = \tfrac{1}{2}(a_{n-2} + a_n). \tag{21g}$$

Substituting (21g) into (21f) and then solving for a_n gives

$$a_n = \gamma a_{n-3} + \delta a_{n-2}, \tag{21h}$$

where

$$\gamma = -\frac{N'''_{n-3}(L)}{\frac{1}{2}N'''_{n-1}(L) + N'''_n(L)}, \qquad \delta = -\frac{N'''_{n-2}(L) + \frac{1}{2}N'''_{n-1}(L)}{\frac{1}{2}N'''_{n-1}(L) + N'''_n(L)}. \tag{21i}$$

For each collocation point, by virtue of (21g) and (21h), the expression $\sum_{j=1}^n k_{ij}a_j$ is finally written as

$$\sum_{j=1}^n k_{ij}a_j = \ldots + k_{i,n-4}a_{n-4} + \underbrace{\left(k_{i,n-3} + \tfrac{1}{2}\gamma k_{i,n-1} + \gamma k_{i,n}\right)}_{\hat{k}_{i,n-3}} a_{n-3} + \underbrace{\left(k_{i,n-2} + \tfrac{1}{2}(1+\delta)k_{i,n-1} + \delta k_{i,n}\right)}_{\hat{k}_{i,n-2}} a_{n-2}. \tag{22}$$

Equation (22) dictates the algorithm which has to be followed for imposing the natural b.c. at the free end B. In brief, the last two columns of the initial matrices (K, M) should be deleted, but before performing this task a linear combination of their elements should be added to the initial $(n-3)$-th and $(n-2)$-th columns according to (22).

As an example, in the particular case of Bézier (Bernstein) polynomials $B_{i,n}(x) = \binom{n}{i}x^i(1-x)^{n-1}$, which is the simplest B-spline in the interval $[0, 1]$, it is trivial to prove that

$$B'''_{n-3,n}(1) = -\alpha, \ B'''_{n-2,n}(1) = 3\alpha, \ B'''_{n-1,n}(1) = -3\alpha, \ B'''_{n,n}(1) = \alpha, \quad \text{with } \alpha = n(n-1)(n-2), \tag{23a}$$

$$B''_{n-3,n}(1) = 0, \quad B''_{n-2,n}(1) = \beta, \quad B''_{n-1,n}(1) = -2\beta, \ B''_{n,n}(1) = \beta, \quad \text{with } \beta = n(n-1), \tag{23b}$$

$$B'_{n-3,n}(1) = 0, \quad B'_{n-2,n}(1) = 0, \quad B'_{n-1,n}(1) = -n, \quad B'_{n,n}(1) = n; \tag{23c}$$

hence, $\gamma = -2$ and $\delta = 3$.

Let us now leave beams and return to real plates. In the case of a *clamped* plate, those columns of matrices (M, K) that correspond to the two layers of control points, which are the closest ones to the boundary, should be deleted. The explanation is the same as that for the clamped point A of the above-mentioned cantilever beam (i.e., by virtue of (21c) and (21d), perpendicularly to the boundary).

In the particular case of a *simply supported* plate, first all columns that correspond to the outermost control points will be deleted. Second, since the normal moment vanishes ($M_n = 0$), the current situation is very similar to (21e), and the concept of (22) can be applied as is.

In the general case of a 2-D plate with arbitrary boundary conditions, the above procedure is generalized as follows. In compact form, the imposition of Neumann b.c. can be written in the form

$$[A_{22} \ A_{2i}] \begin{Bmatrix} a_2 \\ a_i \end{Bmatrix} = \{0\}, \tag{24}$$

where the elements of the matrices A_{22} and A_{2i} include second and third directional derivatives of the basis functions. The vector a_2 refers to the generalized coefficients that are related to the control points on the Neumann boundary, whereas the vector a_i refers to inner ones.

In the free vibration problem, (6) can be written as

$$[M_{c2} \ M_{ci}] \begin{Bmatrix} \ddot{a}_2 \\ \ddot{a}_i \end{Bmatrix} + [K_{c2} \ K_{ci}] \begin{Bmatrix} a_2 \\ a_i \end{Bmatrix} = \{0\}. \tag{25}$$

Solving (24) in a_2 and then substituting into (25), one finally obtains the standard expression

$$\bar{M}\ddot{a}_i + \bar{K}a_i = \mathbb{0} \tag{26}$$

where

$$\bar{M} = M_{ci} - M_{c2}(A_{22})^{-1}A_{2i}, \qquad \bar{K} = K_{ci} - K_{c2}(A_{22})^{-1}A_{2i}. \tag{27}$$

5. Handling the curved boundaries

The proposed method is based on isoparametric considerations. Therefore the tensor product, which describes the flexure of the plate according to (2), is considered to describe the curved geometry as well. As usual, natural coordinates (ξ, η) normalized in the interval [0, 1] have to be considered.

In general, the analyst has to choose the four corner points (i.e., A, B, C and D, shown in Figure 1, right) on the real curvilinear boundary of the plate, and then define the number and the position of the breakpoints along the four curvilinear parts AB, BC, CD and DA on the boundary, as well as the polynomial degree p. Every collocation point corresponds to a specific pair (ξ, η), which is known in advance.

For the arbitrary curved plate with given collocation points, while the mass matrix continues to be described by the simple product of (5), the fourth-order operator of a shape function (i.e., $\nabla^4 N(x, y) = \partial^4 N/\partial x^4 + 2\,\partial^4 N/\partial x^2\partial y^2 + \partial^4 N/\partial y^4$) is more difficult to compute. Concretely, the computation of the stiffness matrix demands the transformation of $\nabla^4 N(x, y)$ in ξ- and η-coordinates, as outlined in the Appendix.

6. Numerical results

The proposed theory is thoroughly evaluated in two benchmark problems that concern a square thin plate of dimensions $a \times a$ under two different boundary conditions. In addition, at the end of this section, the applicability of the proposed method is shown for a circular plate as well. The first problem refers to a simply supported square plate (SS) whereas the second to a clamped (CL) one. In both cases the numerical solution is compared with:

(1) The previous *cubic B-splines Galerkin–Ritz formulation* [Antes 1974] implemented with a standard 4×4 Gaussian quadrature scheme in an in-house computer code, and

(2) the conventional *finite element method* (FEM) using element SHELL63 of ANSYS version 14.5 on a uniform mesh that coincides with the uniform mesh of breakpoints utilized in the global collocation solution.

(3) The *exact solution*, which is given as [Leissa 1973]

$$f_{ij}[\text{Hz}] = \frac{\lambda_{ij}^2}{2\pi a^2}\left[\frac{Eh^2}{12\rho(1 - v^2)}\right]^{1/2}; \quad i = 1, 2, 3\ldots;\ j = 1, 2, 3\ldots, \tag{28}$$

where i and j are the numbers of half-waves in mode shape along x and y axis, respectively, and λ_{ij}^2 is a parameter that depends on the ratio (a/b) of the length over the width of the plate as well as on the type of boundary conditions according to Table 1.

Concerning the proposed global collocation method, we remind that, for a polynomial degree $p = 5$, 6 or 7, then 2×2, 3×3 or 4×4 collocation points per cell (of breakpoints) are chosen, respectively.

type of boundary conditions	λ_{ij}^2 (mode)					
	1	2	3	4	5	6
simply supported [Leissa 1973]	$2\pi^2$ (1, 1)	$5\pi^2$ (2, 1)	$5\pi^2$ (1, 2)	$8\pi^2$ (2, 2)	$10\pi^2$ (3, 1)	$10\pi^2$ (1, 3)
fully clamped [Wieners 1997, p. 38]	35.9852 (1, 1)	73.3938 (2, 1)	73.3938 (1, 2)	108.2165 (2, 2)	131.5808 (3, 1)	132.2048 (1, 3)

Table 1. The values of parameter λ_{ij}^2 and the numbers (i, j) of half-waves for a square plate in bending.

The computational results are presented in the form of errors (in percent, %) of the eigenvalue, $\omega_{ij}^2 = (2\pi f_{ij})^2$:

$$\text{Error}(\%) = \frac{\|\omega_{\text{calculated}}^2 - \omega_{\text{exact}}^2\|}{\omega_{\text{exact}}^2} \times 100. \tag{29}$$

Example 1 (Simply supported rectangular plate). Depending on the polynomial degree, the results illustrated in Figure 3 show an excellent convergence in terms of mesh density. It is noted that when $p = 5$ (not shown), the global collocation method converges somewhat slower than the FEM solution. In contrast, Figure 3 shows that when $p = 6$ or 7 the numerical solution becomes extremely accurate even when treating the entire plate as a unique cell.

Example 2 (Clamped rectangular plate). Similar results were found in this example as well (see Figure 4). It is noted that the exact solution was taken according to Wieners [1997], who presents more decimal digits than Leissa [1973].

Finally, we show how the particular choice of collocation points affects the solution. Let the knot vector, see (7), be written as $V = \{v_1, \ldots, v_{n+p+1}\}$, where n is the number of control points. Except for the above-mentioned Gaussian points, more sets were determined as follows:

(1) "Demko" abscissae were determined on the basis of "p-2" degree. We used the MATLAB command *chbpnt(knotsx(4:length(knotsx)-3),k-2)*. This way leads to the same number of collocation points as obtained using Gaussian points. It is noted that neither the first abscissa is zero nor the last one is equal to the unit.

(2) "Greville-1" abscissae were again determined on the basis of "p-2" degree. The first four knots were not considered.

(3) "Greville-2" abscissae were now determined on the basis of "p" degree. The first three knots were not considered, and all produced abscissae were used.

Concerning the two first sets (i.e., Demko and Greville-1), it is noted that unlike the second order problems (see [Auricchio et al. 2010; Provatidis 2014]), neither the first abscissa is zero nor the last one is equal to the unit.

The performance of the above-mentioned abscissae as collocation points is shown in Figure 5. One may observe that while for $p = 6$ the Gaussian points are competitive with Demko's abscissae, in contrast
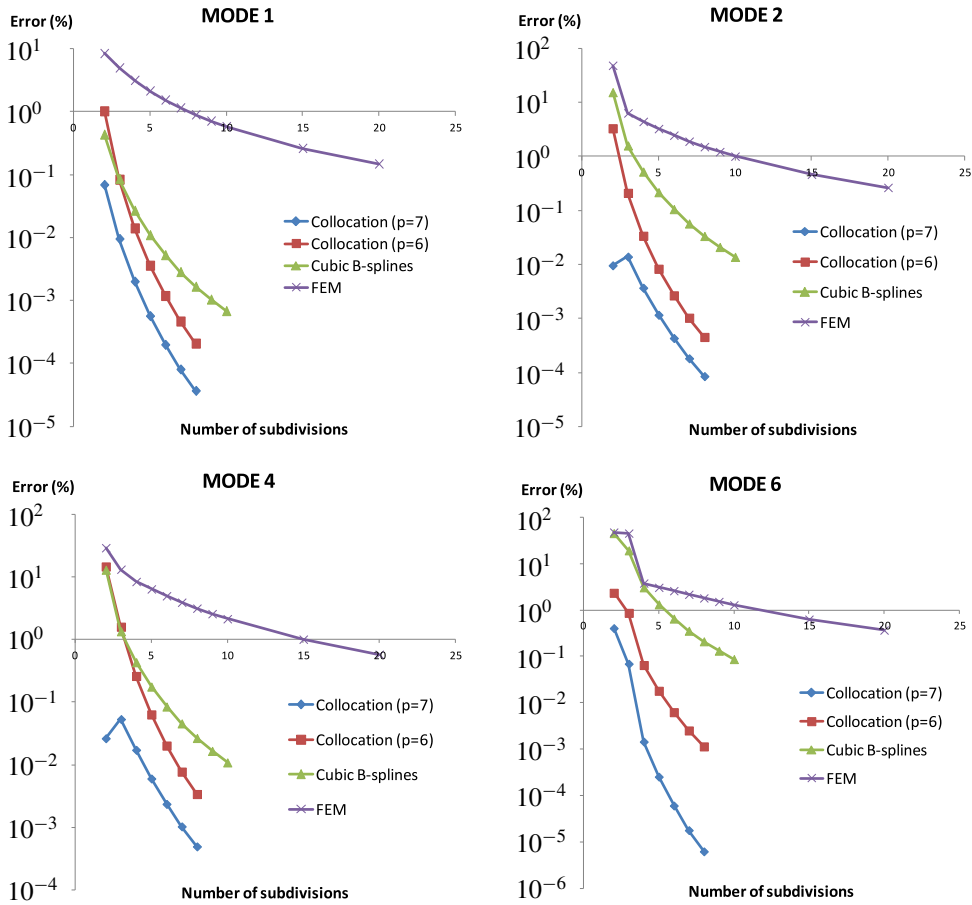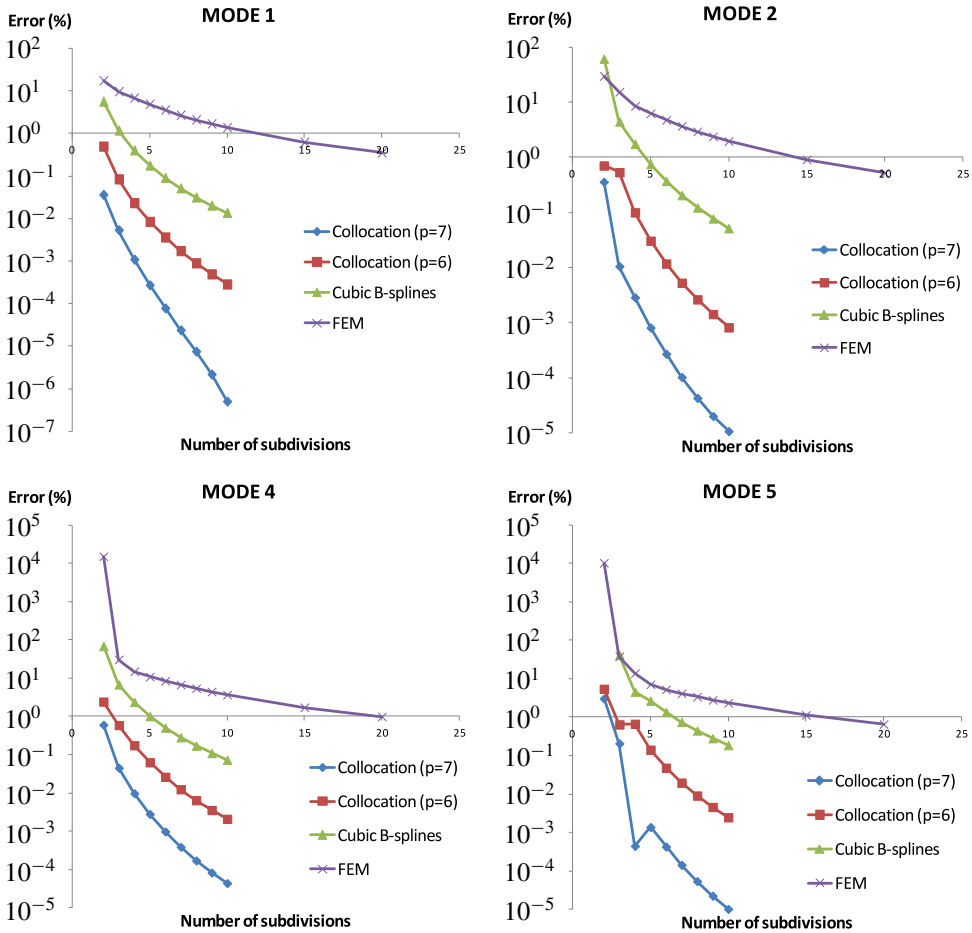
Figure 3. Convergence quality of the first calculated eigenvalues for a simply supported square plate.

to $p = 7$, these are rather superior. Between the two Greville-type abscissae, Greville-2 (based on p-th degree) is superior.

Example 3 (Circular clamped plate). A circular clamped plate of radius $R = 1$ was analyzed and the proposed collocation method was successfully compared with the exact solution [Zhou et al. 2011]. Table 2 presents the numerical results when the collocation points are taken at the location of the Gaussian points. One may observe the excellent and rapid convergence towards the exact solution. It is noted that the minor error that appears at the first natural frequency is probably due to the insufficient number of digital points that literature presents, a matter that has been extensively discussed in [Zhou et al. 2011]. Moreover, the number of equations is shown at the bottom of Table 2.

Concerning conventional plate finite elements (structured mesh using three different types from AN-SYS library), the convergence rate is very slow and the error of the first natural eigenfrequency is considerably greater than that of the proposed collocation method (Table 2), as clearly shown in Table 3.

Figure 4. Convergence quality of the first calculated eigenvalues for a clamped square plate.

Regarding the other nine modes, the error is practically maintained at the same level with the first one, thus they are not shown.

7. Discussion

As previously reported in the case of 2-D acoustics [Provatidis 2014], the accuracy of the proposed B-splines collocation method in plate-bending eigenvalue analysis is again excellent. An interesting finding is that in the first two examples (square plate) of this study, the proposed global collocation method converges from lower to higher values, exactly as the FEM (ANSYS) solution behaves. It is noted that similar results with ANSYS (of slightly lower quality) were obtained using an in-house code that implemented the shape functions of the well-known MZC 12-DOF finite element [Melosh 1963] in conjunction with a consistent mass formulation. Therefore, the quality of the general purpose commercial software (one of the most reliable worldwide) or the particular choice of the SHELL63 is not to be
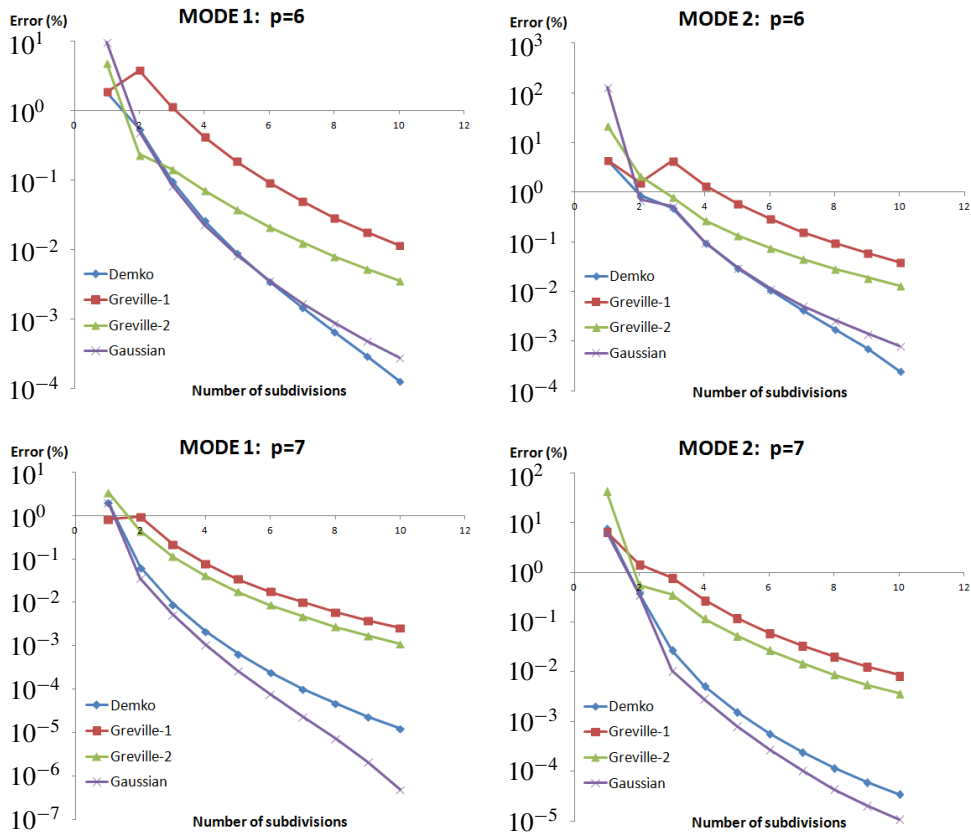
Figure 5. Influence of each particular set of collocation points on the first two eigenvalues for a clamped square plate.

blamed. The superiority of the proposed method is mainly due to the high polynomial degree of the flexural approximation.

Tables 2 and 3 show that for the circular clamped plate, the pattern of convergence is not as clear as it was for the square one, whereas even the three ANSYS types of elements tested also have different convergence patterns, although they converge to very similar values.

The above-mentioned procedure leads to excellent results but is strictly related to the proposed number of collocation points according to (16)–(19). In principle, an alternative could be to use a Lagrange multiplier scheme according to which the boundary condition at the Neumann part of the boundary is properly added to the equation related to the fulfillment of the partial differential equation. However, the accuracy of this procedure is out of the scope of this paper. For an analog to in-plane elasticity, the interested reader is referred to the Appendix of [Provatidis 2017].

Although this paper is restricted to B-spline collocation, which is a special case of the so-called *global collocation methods* (GCM), a generalization is possible. In more detail, it is worthy to mention that the high polynomial degree in the B-splines representation and the closely related high accuracy in the obtained numerical results characterize all other CAD-based formulations as well. Specifically, B-splines approximation is chronologically the fourth main "station" in CAD history [Provatidis 2014].

mode	λ_{ij}^2	$p = 6$ number of knot spans				$p = 7$ number of knot spans			
		2	3	4	6	1	2	3	4
1	10.2158	0.91	−0.03	0.03	0.03	7.17	−0.02	0.04	0.03
2	21.2604	1.31	0.50	−0.03	0.01	−8.04	−0.23	−0.01	0.01
3	21.2604	1.33	0.52	−0.01	0.02	−8.02	−0.22	0.00	0.03
4	34.8770	−7.55	−0.07	−0.14	0.02	−21.83	−0.89	−0.03	−0.02
5	34.8770	4.32	0.96	0.62	0.02	277.49	3.34	0.03	0.02
6	39.7711	−6.96	−0.00	0.62	0.02	262.93	3.31	0.04	−0.02
7	51.0306	−1.49	0.74	0.32	0.01	217.25	1.91	−0.00	0.00
8	51.0306	−1.48	0.74	0.32	0.01	217.27	1.91	−0.00	0.00
9	60.8287	3.93	1.83	0.19	−0.03	191.31	2.25	−0.25	0.02
number of equations		36	81	144	324	16	64	144	256

Table 2. Errors (in %) of the calculated natural frequencies for a clamped circular plate of unit radius. Natural frequencies were calculated using the proposed B-splines collocation method based on the Gaussian points, for piecewise polynomial degrees $p = 6$ and 7. For the exact parameter λ_{ij}^2, see (28).

element type (ANSYS)	number of circumferential uniform segments per quarter of the circle ($n_\xi = n_\eta$)			
	8	16	32	64
SHELL43	6.55	4.13	3.57	3.43
SHELL63	2.44	3.14	3.34	3.39
SHELL181	10.02	4.97	3.77	3.47
number of unrestrained nodal points	49	225	961	3969
number of equations	147	675	2883	11907

Table 3. Errors (in %) of the calculated first natural frequency for a clamped circular plate of unit radius. This demonstrates the quality of the calculated first natural frequency using several types of finite elements (ANSYS library). Value for the exact parameter λ_{ij}^2, see (28), is 10.2158. For the number of equations, all equations have unrestrained bending DOF, excepting the membrane behavior.

Taking the mid-1960s as a starting point, the five consecutive stations in CAD approximation theory are (see, for example, [Farin et al. 2002]):

 (1) Coons interpolation (in 1967),

 (2) Gordon transfinite interpolation (in 1970),

 (3) Bézier curves,

(4) B-splines and

(5) NURBS.

In general, and independently on the governing partial differential equation, the boundary value or the eigenvalue problem can be solved using one of the aforementioned five CAD-based approximations, and one of the basic computational methods: Ritz–Galerkin, boundary element and collocation, among others. These fifteen combinations increase by a factor equal to two when considering triangular patches (Barnhill's approximation: one more CAD-station) in addition to the quadrilateral ones.

Let us examine the above-mentioned four interpolations, one-by-one:

(1) Concerning the *boundary-only* Coons interpolation (first CAD-station), the GCM is not applicable at all. The reason is due to the elimination of all boundary DOF, a matter discussed in detail elsewhere [Provatidis 2014]. In contrast, the same interpolation performs well in the static plate analysis in conjunction with the Ritz–Galerkin formulation [Provatidis and Angelidis 2014].

(2) Although numerical results were not presented, the GCM performs well in conjunction with the *transfinite* interpolation (second CAD-station). Similarly, transfinite interpolation performs well in conjunction with the Ritz–Galerkin formulation [Provatidis 2008c]. This is due to the existence of internal nodes that raise the accuracy of the approximation.

(3) Although not mentioned so far, the numerical results of this paper include the Bézier interpolation (third CAD-station) as well. This happens because when using one subdivision of each side (shown by the left extreme points in Figures 3 and 4), B-spline degenerates to Bernstein polynomials.

(4) B-splines collocation performed well (see Figures 3 and 4). Similarly, when B-splines approximation is applied in conjunction with the Ritz–Galerkin formulation (not presented), the quality of the numerical solution is high, as summarized in [Höllig 2003].

8. Conclusions

It was shown that the proposed global collocation method has excellent performance in the eigenvalue analysis of simply supported and clamped plates. For a specified number of uniformly arranged breakpoints, the procedure is more accurate than the conventional finite element method as well as the cubic B-splines Galerkin–Ritz formulation. Although results were presented for only the eigenvalue problem, the static analysis shows a similar behavior. When the structure is of complex shape, it is suggested to subdivide it into large macroelements of regular shape and apply compatibility and equilibrium conditions along the interfaces. A similar behavior is anticipated for shell structures.

Appendix: The biharmonic function in the (ξ, η)-space

For each collocation point $P(\xi, \eta)$, which is known in the unit square of a reference (ξ, η)-plane, the proposed method needs to handle the Cartesian coordinates in the form $x(\xi, \eta)$ and $y(\xi, \eta)$. Since the global shape functions $N(x, y)$, which appear in (3), are tensor products of univariate basis functions (here, B-splines) that are known in the (ξ, η)-space, the biharmonic operator

$$\nabla^4 N(x, y) = \frac{\partial^4 N(x, y)}{\partial x^4} + 2 \frac{\partial^4 N(x, y)}{\partial x^2 \partial y^2} + \frac{\partial^4 N(x, y)}{\partial y^4}, \tag{A.1}$$

has to be transformed from x and y into ξ and η.

This is accomplished first by calculating the Jacobian matrix $\boldsymbol{J} = \begin{bmatrix} \partial x/\partial \xi & \partial y/\partial \xi \\ \partial x/\partial \eta & \partial y/\partial \eta \end{bmatrix}$ at the collocation point $P(x(\xi, \eta), y(\xi, \eta))$. Then, by numerical inversion, the four terms of its inverse $\boldsymbol{J}^{-1}$ are found:

$$\boldsymbol{J}^{-1} = \begin{bmatrix} \dfrac{\partial \xi}{\partial x} & \dfrac{\partial \eta}{\partial x} \\[2ex] \dfrac{\partial \xi}{\partial y} & \dfrac{\partial \eta}{\partial y} \end{bmatrix}. \tag{A.2}$$

Second, every term that appears in (A.1) is processed in a systematic way as follows. The chain rule is successively applied on an arbitrary continuous and differentiable function $F(x, y)$, whence the following three principal formulas are derived:

$$\frac{\partial^2 F}{\partial x^2} = \frac{\partial^2 F}{\partial \xi^2}\left(\frac{\partial \xi}{\partial x}\right)^2 + 2\frac{\partial^2 F}{\partial \xi \partial \eta}\frac{\partial \xi}{\partial x}\frac{\partial \eta}{\partial x} + \frac{\partial^2 F}{\partial \eta^2}\left(\frac{\partial \eta}{\partial x}\right)^2 + \frac{\partial F}{\partial \xi}\frac{\partial^2 \xi}{\partial x^2} + \frac{\partial F}{\partial \eta}\frac{\partial^2 \eta}{\partial x^2}, \tag{A.3}$$

$$\frac{\partial^2 F}{\partial x \partial y} = \frac{\partial^2 F}{\partial \xi^2}\frac{\partial \xi}{\partial x}\frac{\partial \xi}{\partial y} + \frac{\partial^2 F}{\partial \xi \partial \eta}\left(\frac{\partial \xi}{\partial x}\frac{\partial \eta}{\partial y} + \frac{\partial \xi}{\partial y}\frac{\partial \eta}{\partial x}\right) + \frac{\partial^2 F}{\partial \eta^2}\frac{\partial \eta}{\partial x}\frac{\partial \eta}{\partial y} + \frac{\partial F}{\partial \xi}\frac{\partial^2 \xi}{\partial x \partial y} + \frac{\partial F}{\partial \eta}\frac{\partial^2 \eta}{\partial x \partial y}, \tag{A.4}$$

$$\frac{\partial^2 F}{\partial y^2} = \frac{\partial^2 F}{\partial \xi^2}\left(\frac{\partial \xi}{\partial y}\right)^2 + 2\frac{\partial^2 F}{\partial \xi \partial \eta}\frac{\partial \xi}{\partial y}\frac{\partial \eta}{\partial y} + \frac{\partial^2 F}{\partial \eta^2}\left(\frac{\partial \eta}{\partial y}\right)^2 + \frac{\partial F}{\partial \xi}\frac{\partial^2 \xi}{\partial y^2} + \frac{\partial F}{\partial \eta}\frac{\partial^2 \eta}{\partial y^2}. \tag{A.5}$$

It is noted that (A.3) and (A.5) have previously assisted the implementation of the collocation method in potential (Laplace and Poisson) type problems [Provatidis 2009].

As a third step in the above equations (A.3), (A.4), and (A.5), the arbitrary function F is replaced by the shape function N, thus respectively yielding

$$\frac{\partial^2 N}{\partial x^2} = \frac{\partial^2 N}{\partial \xi^2}\left(\frac{\partial \xi}{\partial x}\right)^2 + 2\frac{\partial^2 N}{\partial \xi \partial \eta}\frac{\partial \xi}{\partial x}\frac{\partial \eta}{\partial x} + \frac{\partial^2 N}{\partial \eta^2}\left(\frac{\partial \eta}{\partial x}\right)^2 + \frac{\partial N}{\partial \xi}\frac{\partial^2 \xi}{\partial x^2} + \frac{\partial N}{\partial \eta}\frac{\partial^2 \eta}{\partial x^2}, \tag{A.6}$$

$$\frac{\partial^2 N}{\partial x \partial y} = \frac{\partial^2 N}{\partial \xi^2}\frac{\partial \xi}{\partial x}\frac{\partial \xi}{\partial y} + \frac{\partial^2 N}{\partial \xi \partial \eta}\left(\frac{\partial \xi}{\partial x}\frac{\partial \eta}{\partial y} + \frac{\partial \xi}{\partial y}\frac{\partial \eta}{\partial x}\right) + \frac{\partial^2 N}{\partial \eta^2}\frac{\partial \eta}{\partial x}\frac{\partial \eta}{\partial y} + \frac{\partial N}{\partial \xi}\frac{\partial^2 \xi}{\partial x \partial y} + \frac{\partial N}{\partial \eta}\frac{\partial^2 \eta}{\partial x \partial y}, \tag{A.7}$$

$$\frac{\partial^2 N}{\partial y^2} = \frac{\partial^2 N}{\partial \xi^2}\left(\frac{\partial \xi}{\partial y}\right)^2 + 2\frac{\partial^2 N}{\partial \xi \partial \eta}\frac{\partial \xi}{\partial y}\frac{\partial \eta}{\partial y} + \frac{\partial^2 N}{\partial \eta^2}\left(\frac{\partial \eta}{\partial y}\right)^2 + \frac{\partial N}{\partial \xi}\frac{\partial^2 \xi}{\partial y^2} + \frac{\partial N}{\partial \eta}\frac{\partial^2 \eta}{\partial y^2}. \tag{A.8}$$

As a fourth step, the function F in (A.3) is replaced by $\partial^2 N/\partial x^2$ in the form of (A.6); in this way the term $\partial^4 N/\partial x^4$ is produced. Similarly, the function F in (A.4) is replaced by $\partial^2 N/\partial x \partial y$ in the form of (A.7), thus the term $\partial^4 N/\partial x^2 \partial y^2$ is produced. Finally, the function F in (A.5) is replaced by $\partial^2 N/\partial y^2$ in the form of (A.8), thus the final desired term $\partial^4 N/\partial y^4$ is produced.

Since each of (A.3) to (A.5) consists of five terms, the above procedure leads to $5 \times 5 = 25$ fundamental terms. But since all the aforementioned 25 fundamental terms are partial derivatives of rather complicated terms, which are multiples of up to three secondary functions, the further procedure is highly facilitated by systematically adopting the following identity (generalized chain rule):

$$\frac{\partial^2}{\partial \xi \partial \eta}(f \cdot g \cdot h) = \frac{\partial^2 f}{\partial \xi \partial \eta} \cdot g \cdot h + f \cdot \frac{\partial^2 g}{\partial \xi \partial \eta} \cdot h + f \cdot g \cdot \frac{\partial^2 h}{\partial \xi \partial \eta}$$
$$+ \left(\frac{\partial f}{\partial \eta} \cdot \frac{\partial g}{\partial \xi} + \frac{\partial f}{\partial \xi} \cdot \frac{\partial g}{\partial \eta}\right) \cdot h + \left(\frac{\partial f}{\partial \eta} \cdot \frac{\partial h}{\partial \xi} + \frac{\partial f}{\partial \xi} \cdot \frac{\partial h}{\partial \eta}\right) \cdot g + \left(\frac{\partial g}{\partial \eta} \cdot \frac{\partial h}{\partial \xi} + \frac{\partial g}{\partial \xi} \cdot \frac{\partial h}{\partial \eta}\right) \cdot f. \tag{A.9}$$

Obviously, (A.9) covers all necessary cases. For example, when dealing with $\partial^2/\partial\xi^2(fgh)$, one can easily consider that $\eta = \xi$. Also, when dealing with any partial derivative of (fg), one can easily apply (A.9) and taking $h = 1$.

Following the above procedure, rather lengthy expressions are derived. For example, the final result for the first term of (A.1) is given by

$$
\begin{aligned}
\frac{\partial^4 N}{\partial x^4} = {}& \frac{\partial^4 N}{\partial \xi^4} \cdot \left(\frac{\partial \xi}{\partial x}\right)^4 + \frac{\partial^4 N}{\partial \eta^4} \cdot \left(\frac{\partial \eta}{\partial x}\right)^4 + \frac{\partial^4 N}{\partial \xi^3 \partial \eta} \cdot \left[4\left(\frac{\partial \xi}{\partial x}\right)^3 \left(\frac{\partial \eta}{\partial x}\right)\right] + \frac{\partial^4 N}{\partial \xi^2 \partial \eta^2} \cdot \left[6\left(\frac{\partial \xi}{\partial x}\right)^2 \left(\frac{\partial \eta}{\partial x}\right)^2\right] \\
&+ \frac{\partial^4 N}{\partial \xi \partial \eta^3} \cdot \left[4\left(\frac{\partial \xi}{\partial x}\right)\left(\frac{\partial \eta}{\partial x}\right)^3\right] + \frac{\partial^3 N}{\partial \xi^3} \cdot \left[6\left(\frac{\partial \xi}{\partial x}\right)^2 \left(\frac{\partial^2 \xi}{\partial x^2}\right)\right] + \frac{\partial^3 N}{\partial \eta^3} \cdot \left[6\left(\frac{\partial \eta}{\partial x}\right)^2 \left(\frac{\partial^2 \eta}{\partial x^2}\right)\right] \\
&+ \frac{\partial^3 N}{\partial \xi^2 \partial \eta} \cdot \left[12\left(\frac{\partial \xi}{\partial x}\right)\left(\frac{\partial \eta}{\partial x}\right)\left(\frac{\partial^2 \xi}{\partial x^2}\right) + 6\left(\frac{\partial \xi}{\partial x}\right)^2 \left(\frac{\partial^2 \eta}{\partial x^2}\right)\right] \\
&+ \frac{\partial^3 N}{\partial \xi \partial \eta^2} \cdot \left[12\left(\frac{\partial \xi}{\partial x}\right)\left(\frac{\partial \eta}{\partial x}\right)\left(\frac{\partial^2 \eta}{\partial x^2}\right) + 6\left(\frac{\partial \eta}{\partial x}\right)^2 \left(\frac{\partial^2 \xi}{\partial x^2}\right)\right] \\
&+ \frac{\partial^2 N}{\partial \xi^2} \cdot \left[4\left(\frac{\partial \xi}{\partial x}\right)\left(\frac{\partial^3 \xi}{\partial x^3}\right) + 3\left(\frac{\partial^2 \xi}{\partial x^2}\right)^2\right] + \frac{\partial^2 N}{\partial \eta^2} \cdot \left[4\left(\frac{\partial \eta}{\partial x}\right)\left(\frac{\partial^3 \eta}{\partial x^3}\right) + 3\left(\frac{\partial^2 \eta}{\partial x^2}\right)^2\right] \\
&+ \frac{\partial^2 N}{\partial \xi \partial \eta} \cdot \left[4\left(\frac{\partial \xi}{\partial x}\right)\left(\frac{\partial^3 \eta}{\partial x^3}\right) + 4\left(\frac{\partial \eta}{\partial x}\right)\left(\frac{\partial^3 \xi}{\partial x^3}\right) + 6\left(\frac{\partial^2 \xi}{\partial x^2}\right)\left(\frac{\partial^2 \eta}{\partial x^2}\right)\right] \\
&+ \frac{\partial N}{\partial \xi} \cdot \left(\frac{\partial^4 \xi}{\partial x^4}\right) + \frac{\partial N}{\partial \eta} \cdot \left(\frac{\partial^4 \eta}{\partial x^4}\right).
\end{aligned}
\tag{A.10}
$$

One may observe that the right part of (A.10) includes all partial derivatives of the shape function N, starting from the fourth derivative, $\partial^4 N/\partial\xi^4$, and finishing with the first one, $\partial N/\partial\eta$.

References

[Akhras and Li 2011] G. Akhras and W. Li, "Stability and free vibration analysis of thick piezoelectric composite plates using spline finite strip method", *Int. J. Mech. Sci.* **53**:8 (2011), 575–584.

[Antes 1974] H. Antes, "Bicubic fundamental splines in plate bending", *Int. J. Numer. Methods Eng.* **8**:3 (1974), 503–511.

[Auricchio et al. 2010] F. Auricchio, L. Beirão da Veiga, T. J. R. Hughes, A. Reali, and G. Sangalli, "Isogeometric collocation methods", *Math. Models Methods Appl. Sci.* **20**:11 (2010), 2075–2107.

[Bathe 1996] K. J. Bathe, *Finite element procedures*, Prentice-Hall, New Jersey, 1996.

[de Boor 1972] C. de Boor, "On calculating with *B*-splines", *J. Approx. Theory* **6**:1 (1972), 50–62.

[de Boor and Swartz 1973] C. de Boor and B. Swartz, "Collocation at Gaussian points", *SIAM J. Numer. Anal.* **10**:4 (1973), 582–606.

[Cheng and Dade 1990] S. P. Cheng and C. Dade, "Dynamic analysis of stiffened plates and shells using spline gauss collocation method", *Comput. Struct.* **36**:4 (1990), 623–629.

[Cottrell et al. 2009] J. A. Cottrell, T. J. R. Hughes, and Y. Bazilevs, *Isogeometric analysis: towards integration of CAD and FEA*, Wiley, Chichester, England, 2009.

[Dawe and Wang 1995] D. J. Dawe and S. Wang, "Spline finite strip analysis of the buckling and vibration of rectangular composite laminated plates", *Int. J. Mech. Sci.* **37**:6 (1995), 645–667.

[Echter et al. 2013] R. Echter, B. Oesterle, and M. Bischoff, "A hierarchic family of isogeometric shell finite elements", *Comput. Methods Appl. Mech. Eng.* **254** (2013), 170–180.

[Fan and Luah 1995] S. C. Fan and M. H. Luah, "Free vibration analysis of arbitrary thin shell structures by using spline finite element", *J. Sound Vib.* **179**:5 (1995), 763–776.

[Farin et al. 2002] G. Farin, J. Hoschek, and M.-S. Kim (editors), *Handbook of computer aided geometric design*, Elsevier, Amsterdam, 2002.

[Filippatos 2010] A. Filippatos, *Extraction of eigenfrequencies in acoustic cavities and elastic structures using the global collocation method*, Diploma work, National Technical University of Athens, 2010, available at http://users.ntua.gr/cprovat/yliko/Filippatos_Diploma_Thesis.pdf. In Greek.

[Golmakani and Mehrabian 2014] M. E. Golmakani and M. Mehrabian, "Nonlinear bending analysis of ring-stiffened circular and annular general angle-ply laminated plates with various boundary conditions", *Mech. Res. Commun.* **59** (2014), 42–50.

[Grigorenko and Kryukov 1995] Y. M. Grigorenko and N. N. Kryukov, "Solution of problems in the theory of plates and shells using spline functions (survey)", *Prikl. Mekh.* **31**:6 (1995), 3–27. In Russian; translated in *Internat. Appl. Mech.* **31**:6 (1995), 413–434.

[Gupta et al. 1991] A. Gupta, J. Kiusalaas, and M. Saraph, "Cubic B-spline for finite element analysis of axisymmetric shells", *Comput. Struct.* **38**:4 (1991), 463–468.

[Han et al. 2007] J.-G. Han, W.-X. Ren, and Y. Huang, "A wavelet-based stochastic finite element method of thin plate bending", *Appl. Math. Model.* **31**:2 (2007), 181–193.

[Höllig 2003] K. Höllig, *Finite element methods with B-splines*, Frontiers in Applied Mathematics **26**, Society for Industrial and Applied Mathematics, Philadelphia, 2003.

[Hughes et al. 2010] T. J. R. Hughes, A. Reali, and G. Sangalli, "Efficient quadrature for NURBS-based isogeometric analysis", *Comput. Methods Appl. Mech. Eng.* **199**:5–8 (2010), 301–313.

[Kapoor and Kapania 2012] H. Kapoor and R. K. Kapania, "Geometrically nonlinear NURBS isogeometric finite element analysis of laminated composite plates", *Compos. Struct.* **94**:12 (2012), 3434–3447.

[Kolli and Chandrashekhara 1997] M. Kolli and K. Chandrashekhara, "Non-linear static and dynamic analysis of stiffened laminated plates", *Int. J. Non-Linear Mech.* **32**:1 (1997), 89–101.

[Leissa 1973] A. W. Leissa, "The free vibration of rectangular plates", *J. Sound Vib.* **31**:3 (1973), 257–293.

[Li and Chen 2014] B. Li and X. Chen, "Wavelet-based numerical analysis: a review and classification", *Finite Elem. Anal. Des.* **81** (2014), 14–31.

[Melosh 1963] R. J. Melosh, "Basis for derivation of matrices for the direct stiffness method", *AIAA J.* **1**:7 (1963), 1631–1637.

[Park et al. 2008] T. Park, S.-Y. Lee, J. W. Seo, and G. Z. Voyiadjis, "Structural dynamic behavior of skew sandwich plates with laminated composite faces", *Compos. B Eng.* **39**:2 (2008), 316–326.

[Patlashenko and Weller 1995] I. Patlashenko and T. Weller, "Two-dimensional spline collocation method for nonlinear analysis of laminated panels", *Comput. Struct.* **57**:1 (1995), 131–139.

[Peng-Cheng et al. 1987] S. Peng-Cheng, H. Dade, and W. Zongmu, "Static, vibration and stability analysis of stiffened plates using B spline functions", *Comput. Struct.* **27**:1 (1987), 73–78.

[Piegl and Tiller 1995] L. Piegl and W. Tiller, *The NURBS Book*, Springer, Berlin, 1995.

[Provatidis 2004] C. G. Provatidis, "Coons-patch macroelements in two-dimensional eigenvalue and scalar wave propagation problems", *Comput. Struct.* **82**:4–5 (2004), 383–395.

[Provatidis 2006] C. G. Provatidis, "Transient elastodynamic analysis of two-dimensional structures using Coons-patch macroelements", *Int. J. Solids Struct.* **43**:22–23 (2006), 6688–6706.

[Provatidis 2008a] C. G. Provatidis, "Free vibration analysis of elastic rods using global collocation", *Arch. Appl. Mech.* **78**:4 (2008), 241–250.

[Provatidis 2008b] C. G. Provatidis, "Global collocation method for 2-D rectangular domains", *J. Mech. Mater. Struct.* **3**:1 (2008), 185–194.

[Provatidis 2008c] C. G. Provatidis, "Plate bending analysis using transfinite interpolation", in *6th GRACM International Congress on Computational Mechanics* (Thessaloniki, 2008), edited by D. Talaslidis et al., Sofia Publishers, Thessaloniki, 2008. CD version published by VK-4M Civil Engineering Software Company, Athens.

[Provatidis 2009] C. G. Provatidis, "Integration-free Coons macroelements for the solution of 2D Poisson problems", *Int. J. Numer. Methods Eng.* **77**:4 (2009), 536–557.

[Provatidis 2012] C. G. Provatidis, "Two-dimensional elastostatic analysis using Coons–Gordon interpolation", *Meccanica (Milano)* **47**:4 (2012), 951–967.

[Provatidis 2013] C. G. Provatidis, "A review on attempts towards CAD/CAE integration using macroelements", *Comput. Res.* **1**:3 (2013), 61–84.

[Provatidis 2014] C. G. Provatidis, "B-splines collocation eigenanalysis of 2D acoustic problems", *J. Mech. Mater. Struct.* **9**:3 (2014), 259–285.

[Provatidis 2017] C. G. Provatidis, "CAD-based collocation eigenanalysis of 2-D elastic structures", *Comput. Struct.* **182** (2017), 55–73.

[Provatidis and Angelidis 2014] C. G. Provatidis and D. I. Angelidis, "Performance of Coons' macroelements in plate bending analysis", *Int. J. Comput. Methods Eng. Sci. Mech.* **15**:2 (2014), 110–125.

[Provatidis and Ioannou 2010] C. G. Provatidis and K. S. Ioannou, "Static analysis of two-dimensional elastic structures using global collocation", *Arch. Appl. Mech.* **80**:4 (2010), 389–400.

[Reddy and Palaninathan 1999] A. R. K. Reddy and R. Palaninathan, "Free vibration of skew laminates", *Comput. Struct.* **70**:4 (1999), 415–423.

[Tran et al. 2013] L. V. Tran, A. J. M. Ferreira, and H. Nguyen-Xuan, "Isogeometric analysis of functionally graded plates using higher-order shear deformation theory", *Compos. B Eng.* **51** (2013), 368–383.

[Valizadeh et al. 2013] N. Valizadeh, S. Natarajan, O. A. Gonzalez-Estrada, T. Rabczuk, T. Q. Bui, and S. P. A. Bordas, "NURBS-based finite element analysis of functionally graded plates: static bending, vibration, buckling and flutter", *Compos. Struct.* **99** (2013), 309–326.

[Wieners 1997] C. Wieners, "Bounds for the *N* lowest eigenvalues of fourth-order boundary value problems", *Computing* **59**:1 (1997), 29–41.

[Zhang et al. 2010] X. Zhang, X. Chen, X. Wang, and Z. He, "Multivariable finite elements based on B-spline wavelet on the interval for thin plate static and vibration analysis", *Finite Elem. Anal. Des.* **46**:5 (2010), 416–427.

[Zhou et al. 2011] Z. H. Zhou, K. W. Wong, X. S. Xu, and A. Y. T. Leung, "Natural vibration of circular and annular thin plates by Hamiltonian approach", *J. Sound Vib.* **330**:5 (2011), 1005–1017.

CHRISTOPHER G. PROVATIDIS: cprovat@central.ntua.gr
School of Mechanical Engineering, National Technical University of Athens, Heroon Polytechniou 9, Zografou Campus, 15780 Athens, Greece

msp

JOURNAL OF MECHANICS OF MATERIALS AND STRUCTURES

Founded by Charles R. Steele and Marie-Louise Steele

Cover photo: Mando Gomez, www.mandolux.com

Journal of Mechanics of Materials and Structures

Volume 12, No. 4   July 2017